DOI: 10.1534/genetics.108.088435

Pleiotropic Effects of Drosophila *neuralized* on Complex Behaviors and Brain Structure

Stephanie M. Rollmann,*,†,1,2 Liesbeth Zwarts,‡,1 Alexis C. Edwards,†,§ Akihiko Yamamoto,*,† Patrick Callaerts,‡ Koenraad Norga,‡, Trudy F. C. Mackay†,§ and Robert R. H. Anholt*,†,§,3**

**Department of Zoology, North Carolina State University, Raleigh, North Carolina 27695-7617, †W. M. Keck Center for Behavioral Biology, North Carolina State University, Raleigh, North Carolina 27695-7617, ‡Laboratory of Developmental Genetics, VIB-PRJ8 and Katholieke Universiteit Leuven, Center for Human Genetics, B-3000 Leuven, Belgium, §Department of Genetics, North Carolina State University, Raleigh, North Carolina 27695-7614 and **Children's Hospital, Katholieke Universiteit Leuven, B-3000 Leuven, Belgium*

Manuscript received February 23, 2008
Accepted for publication April 24, 2008

ABSTRACT

Understanding how genotypic variation influences variation in brain structures and behavioral phenotypes represents a central challenge in behavioral genetics. In *Drosophila melanogaster*, the *neuralized* (*neur*) gene plays a key role in development of the nervous system. Different *P*-element insertional mutations of *neur* allow the development of viable and fertile adults with profoundly altered behavioral phenotypes that depend on the exact location of the inserted *P* element. The *neur* mutants exhibit reduced responsiveness to noxious olfactory and mechanosensory stimulation and increased aggression when limited food is presented after a period of food deprivation. These behavioral phenotypes are correlated with distinct structural changes in integrative centers in the brain, the mushroom bodies, and the ellipsoid body of the central complex. Transcriptional profiling of *neur* mutants revealed considerable overlap among ensembles of coregulated genes in the different mutants, but also distinct allele-specific differences. The diverse phenotypic effects arising from nearby *P*-element insertions in *neur* provide a new appreciation of the concept of allelic effects on phenotype, in which the wild type and null mutant are at the extreme ends of a continuum of pleiotropic allelic effects.

BEHAVIORS are complex traits. Their manifestation depends on interactions among multiple genes and their interplay with the environment. In contrast to other complex traits, behaviors are the quintessential expression of the nervous system, which mediate adaptive responses to changes in the environment. Previous studies have shown that the genetic architectures that shape behaviors are composed of modular ensembles of pleiotropic genes (Anholt *et al.* 2003; Anholt 2004; van Swinderen and Greenspan 2005). Furthermore, subtle disruptions of key genes within such ensembles have widespread effects on transcriptional regulation throughout the genome (Anholt *et al.* 2003) and can display a range of allelic effects that differentially affect different traits (Rollmann *et al.* 2006). For example, nearby *P*-element insertions in the *Tre1-Gr5a* region that interact epistatically with components of the insulin-signaling pathway differentially affect life span, resistance to heat stress and starvation, and preference for trehalose intake (Rollmann *et al.* 2006).

Understanding how genotypic variation results in variation in behavioral phenotypes requires corresponding insights into how variations in structure and function in the nervous system give rise to variation in these behaviors. To begin to understand pleiotropic effects of key genes in epistatic networks that orchestrate behaviors in the context of this "genes–brain–behavior" paradigm, we have studied *P*-element insertional mutants of *neuralized* (*neur*). The *Drosophila melanogaster neur* gene encodes a ubiquitin ligase, which processes the Notch ligand Delta and is involved in cell fate commitment during development of the nervous system (Dietrich and Campos-Ortega 1984; Yeh *et al.* 2000; Lai and Rubin 2001; Lai *et al.* 2001; Pavlopoulos *et al.* 2001; Timmusk *et al.* 2002). *P*-element insertions at *neur* can result in changes in the number of mechanosensory bristles (Norga *et al.* 2003) and reduced olfactory avoidance behavior (Sambandan *et al.* 2006). In addition, lines selected for increased and decreased aggression show altered transcriptional regulation of *neur* compared to unselected lines (Edwards *et al.* 2006).

[1]These authors contributed equally to this work.

[2]*Present address:* Department of Biological Sciences, University of Cincinnati, Cincinnati, OH 45221.

[3]*Corresponding author:* W. M. Keck Center for Behavioral Biology, Campus Box 7617, North Carolina State University, Raleigh, NC 27695-7617. E-mail: anholt@ncsu.edu

We identified three co-isogenic *P*-element insertions in *neur* (Norga *et al.* 2003; Sambandan *et al.* 2006) and studied their effects on olfactory avoidance behavior, aggression, and locomotor reactivity in adult flies. We also performed morphometric neuroanatomical analyses to assess structural changes in integrative centers in the brain, the mushroom bodies, and the ellipsoid body of the central complex. Our observations demonstrate that mutations from nearby *P*-element insertions in a single gene can give rise to pleiotropic behavioral effects associated with neuroanatomical alterations.

MATERIALS AND METHODS

Drosophila stocks: The $neur^{BG02391}$, $neur^{BG02542}$, and $neur^{BG02587}$ *P*-element insertion lines each contain a single *p[GT1]* insertion (Lukacsovich *et al.* 2001; Bellen *et al.* 2004) in the *neur* (*CG11988*) gene region in the co-isogenic Canton-S (B) background. All flies were reared on an agar–yeast–molasses medium in vials at 25° and under a 12-hr light/dark cycle.

***P*-element excision lines:** *P*-element excision lines were constructed in a controlled Canton-S (B) background by crossing *w;CS(B);*$neur^{BG02391}$ or *w;CS(B);*$neur^{BG02542}$ females to *w;Cy/Sp;Sb*Δ*2-3/TM6,Tb* males. Male offspring of the genotype *w;Cy/CS(B);P/Sb*Δ*2-3* were then crossed to *w;CS(B);H/TM3,Sb* females, and single male offspring, *w;CS(B);*P^{-}*/H*, were crossed to *w;CS(B);H/TM3,Sb* females. Progeny in which the *P* element has been excised, *w;CS(B);*P^{-}*/TM3,Sb*, were mated *inter se* to generate a homozygous *P*-element excision line.

Bristle numbers: Abdominal and sternopleural bristle numbers were scored for males and females. Abdominal bristle number is the number of microchaetae on the sixth sternite in females or the fifth sternite in males and sternopleural bristle number reflects the total number of macrochaetae and microchaetae on the right and left sternopleural plates. Four replicates of 10 flies per sex and line were counted. Abdominal and sternopleural bristle numbers were analyzed separately by two-way fixed effects ANOVA according to the model $Y = \mu + L + S + L \times S + E$, where L denotes line, S denotes sex, and E denotes environmental variation. Abdominal bristle number differed by line and sex as shown by a significant line-by-sex interaction term. Thus, abdominal bristle scores were subsequently analyzed separately for each sex according to the ANOVA model $Y = \mu + L + E$, where L denotes line and E denotes environmental variation. Post-hoc Tukey's tests were used to determine significant mean differences among the lines, where applicable.

Behavioral assays: Avoidance responses to benzaldehyde and locomotor reactivity assays were measured as described previously (Anholt *et al.* 1996; Jordan *et al.* 2006; Sambandan *et al.* 2006). Statistically significant differences from the Canton-S (B) control line were evaluated by two-way fixed effects ANOVA according to the model $Y = \mu + L + S + L \times S + E$, where L designates line, S designates sex, and E designates the environmental variation. A post-hoc Tukey's test was used to determine line differences in mean scores, where applicable. Male aggressive behavior was scored using the eight-fly assay described previously by measuring the number of aggressive encounters observed during a 2-min period in an arena with a droplet of food following a period of food deprivation (Edwards *et al.* 2006). Data were analyzed by a one-way fixed effects ANOVA according to the model $Y = \mu + L + E$, where L denotes line and E denotes environmental variation, with a subsequent post-hoc Tukey's test to determine significant mean differences among the lines. All *P*-element insertion lines and the Canton-S (B) control were tested contemporaneously for each behavior, and behavioral data were accumulated over multiple days or weeks to randomize environmental variation. Measurements for each behavior were always made during the same time of day to minimize experimental variation by avoiding differential sampling of circadian fluctuations.

Immunohistochemistry and morphometric analysis: Adult Drosophila brains were fixed in phosphate buffered saline (PBS)–37% formaldehyde for 15 min at room temperature, washed extensively with PBS, and blocked in PAXD [PBS containing 5% bovine serum albumin (Roche Biochemicals), 0.3% Triton X-100, 0.3% sodium deoxycholate] for 10 min at room temperature. Incubation with a 100-fold dilution of antifasciclin II MAb 1D4 (Developmental Studies Hybridoma Bank; under the auspices of the National Institute of Child Health and Human Development and maintained by the University of Iowa, Department of Biological Sciences, Iowa City, IA) was done overnight at 4°. After washing with PAXD, brains were incubated with a 100-fold dilution of Cy™3-conjugated Affinipure goat anti-mouse IgG (H + L) (Jackson ImmunoResearch Laboratories, West Grove, PA) for 2 hr at room temperature, followed by washing with PAXD. Brain samples were mounted in Vectashield mounting medium (Vector Laboratories, Burlingame, CA) and visualized under an Olympus BX61 epifluorescence microscope equipped with a DP70 digital camera controlled with analySIS Software. For ease of analysis, relevant dimensions (length and width of α- and β-lobes and diameters of ellipsoid body; see Figure 2g for color-coded schematic) were measured on screen and were subsequently converted to values (expressed as percentages) relative to the distance between the two mushroom body heels per brain. Statistical significance was determined using two-way ANOVA with post-hoc Tukey's tests. Images for Figure 2, a–d, were generated using a Leica TCS SE confocal laser microscope.

Transcriptional profiling: Flies were frozen on dry ice 5–7 days post eclosion and total RNA was isolated for two replicate groups of males and females for each line. First- and second-strand cDNA were synthesized followed by synthesis of biotinylated cRNA targets. These targets were hybridized to GeneChip Drosophila genome arrays (Affymetrix) and visualized with a streptavidin–phycoerythrin conjugate, as described in the Affymetrix GeneChip Expression Analysis Technical Manual (2000). An estimate of expression of each probe set is the signal metric, which is the weighted averaged signal from all probes within the probe set. Signal values were analyzed by two-way ANOVA according to the model $Y = \mu + L + S + L \times S + E$, where L denotes line, S denotes sex, and E denotes the environmental variation. Corrections for multiple testing were done using the false-discovery-rate q-statistic (Storey and Tibshirani 2003), with a false-discovery-rate threshold for significance set at $q < 0.05$.

Quantitative RT–PCR: RNA was isolated from three replicate groups of 25 animals each of control and *neuralized* mutant adults, as described above. cDNA was generated from 1 μg RNA of each sample using the Transcriptor First Strand cDNA synthesis kit (Roche Biochemicals). The qPCR Mastermix Plus for SYBR Green I (Eurogentec) was used in quantitative RT–PCR (qRT–PCR) reactions that were performed on an ABI7000 instrument. For each replicate group, four technical replicates were measured. Expression levels of transcripts from the various samples were normalized to actin5C expression. We used the following primers: Neur-AB F, 5′-GTCTCGAAGTTGTCGTCGTCGG, and Neur-AB R, 5′-AGCGATAGAGTTCTTCTTCG; Neur-CD F, 5′-GCTCACGGTGCACATAATATCG, and Neur-CD R, 5′-CAGCCACAACAACTAGGACACAC; actin5C F, AGTCCGGCCCCTCCATT, and actin5C R, CTGATCCTCTTGCCCAGACAA. Primers Neur-AB F and

Neur-AB R anneal to exon 2 (shared by transcripts A and B) and will allow quantification of the combined amounts of transcripts A and B, while primers Neur-CD F and Neur-CD R anneal to exon 1 (shared by transcripts C and D) and will allow quantification of the combined amounts of transcripts C and D. Further discrimination between transcripts A *vs.* B and C *vs.* D was technically not possible.

RESULTS

***P*-element insertions at the *neur* locus of *D. melanogaster*:** Drosophila *neur* is a neurogenic gene with a role in cell fate commitment. The Drosophila *neur* gene contains three exons, which generate four alternatively spliced transcripts: *neur*-RA, *neur*-RB, *neur*-RC, and *neur*-RD (NCBI accession no. AE014297). These transcripts differ in the first exon, but share their second and third exons with transcripts *neur*-RA and *neur*-RC differing by 3 bp in the lengths of their second intron and third exon compared to *neur*-RB and *neur*-RD, respectively (Figure 1a). The 3-bp difference is most likely due to alternative splice acceptor site usage. We identified three different *p[GT1]*-element insertions at the *neur* locus ($neur^{BG02391}$, $neur^{BG02542}$, and $neur^{BG02587}$; Bellen *et al.* 2004). The *p[GT1]* insertion sites are ~70 bp upstream of exon 1 of transcripts *neur*-RA and *neur*-RB and in the first intron (~5350 bp downstream of exon 1) of transcripts *neur*-RC and *neur*-RD. All insertions are in the same orientation (Figure 1a).

Previous studies indicated that *neur* mutations can affect numbers of sensory bristles, consistent with the role of *neur* in peripheral nervous system development (Norga *et al.* 2003). We observed a significant reduction of 1.84 sternopleural bristles in homozygous $neur^{BG02391}$ flies in both sexes, but the sternopleural bristle numbers of $neur^{BG02542}$ and $neur^{BG02587}$ were not significantly different from the control (Table 1). The line-by-sex interaction term was significant in the ANOVA of abdominal bristle number ($F_{4,390} = 5.73$, $P = 0.0002$), indicating significant sex-specific effects of *neur* mutations on this trait. $neur^{BG02391}$ males and $neur^{BG02542}$ and $neur^{BG02587}$ females had reduced abdominal bristle numbers compared to the co-isogenic Canton-S (B) control (Table 1).

Pleiotropic behavioral effects of hypomorphic *neur* mutants: In a previous study we demonstrated that $neur^{BG02391}$ homozygotes display decreases in olfactory avoidance behavior in adult flies (Sambandan *et al.* 2006). We confirmed the aberrant olfactory avoidance behavior of $neur^{BG02391}$ mutant flies (Figure 1b). No significant differences in olfactory avoidance behavior from the control were observed for $neur^{BG02542}$ or $neur^{BG02587}$ (data not shown). To verify that the aberrant olfactory phenotype arose due to the insertion of the *p[GT1]* construct rather than from an independent mutation, we mobilized the *p[GT1]* transposon and showed that *P*-element excision restored normal olfactory avoidance behavior (Figure 1b). *P*-element excision also restored the wild-type sternopleural and abdominal bristle phenotype (Table 1).

Next, we asked whether reduced responsiveness to environmental cues was generalized or specific to particular sensory modalities by measuring a startle response (locomotor activity in response to a mechanical stimulus; Jordan *et al.* 2006) and male aggressive behavior (Edwards *et al.* 2006). We observed a significant reduction in locomotor reactivity for both sexes in $neur^{BG02542}$ ($F_{1,116} = 33.45$, $P < 0.0001$) and $neur^{BG02587}$ ($F_{1,116} = 20.47$, $P < 0.0001$) compared to the Canton-S (B) control (Figure 1c). However, $neur^{BG02391}$, which showed reduced olfactory avoidance responses to benzaldehyde, showed normal locomotor reactivity, which indicates that these behavioral phenotypes are dependent on the specific insertion site of the *P* element. To verify that altered locomotor reactivity was indeed attributable to the transposon insertions, we generated two *P*-element excision lines of $neur^{BG02542}$ ($neur^{BG02542Rev1}$ and $neur^{BG02542Rev2}$) and demonstrated restoration of wild-type locomotor reactivity ($F_{3,192} = 14.28$, $P < 0.0001$; Figure 1d).

Surprisingly, the average numbers of aggressive encounters by males competing for a limited food supply after a period of food deprivation were ~1.8-fold greater in $neur^{BG02391}$ and $neur^{BG02587}$ than in the co-isogenic Canton-S (B) control ($F_{2,57} = 20.60$, $P < 0.0001$; Figure 1e). We did not observe a significant effect of $neur^{BG02542}$ on aggressive behavior. Again, *P*-element excision in a controlled genetic background restored the level of aggressive behavior of the $neur^{BG02391}$ mutant to wild-type levels (Figure 1e). The increased level of aggression in these flies demonstrates that their impaired locomotor reactivity is not due to physical limitations on mobility.

Effects of *P*-element insertions in *neur* on brain structure: Olfactory avoidance behavior, startle-induced locomotion, and aggression are behaviors that all involve input from different sensory modalities. This input is integrated and processed in higher brain structures and ultimately results in a motor response. We sought to determine whether the behavioral abnormalities that we observed in *neur* mutant flies could result from structural alterations in integrative centers in the brain, namely the mushroom bodies and the central complex. Sensorimotor coordination in Drosophila depends on the mushroom bodies and the central complex in the brain (Martin *et al.* 1998, 1999). The startle-induced locomotor response is distinct from spontaneous open-field locomotor activity, and not an *a priori* component of aggressive behavior. Thus, the neural circuits that mediate these different behaviors need not necessarily overlap.

In our analysis, we focused on the α- and β-lobes of the mushroom bodies and on the ellipsoid body of the central complex as they integrate information for the execution of complex behaviors. For example, the α-lobes of the mushroom bodies have been implicated in

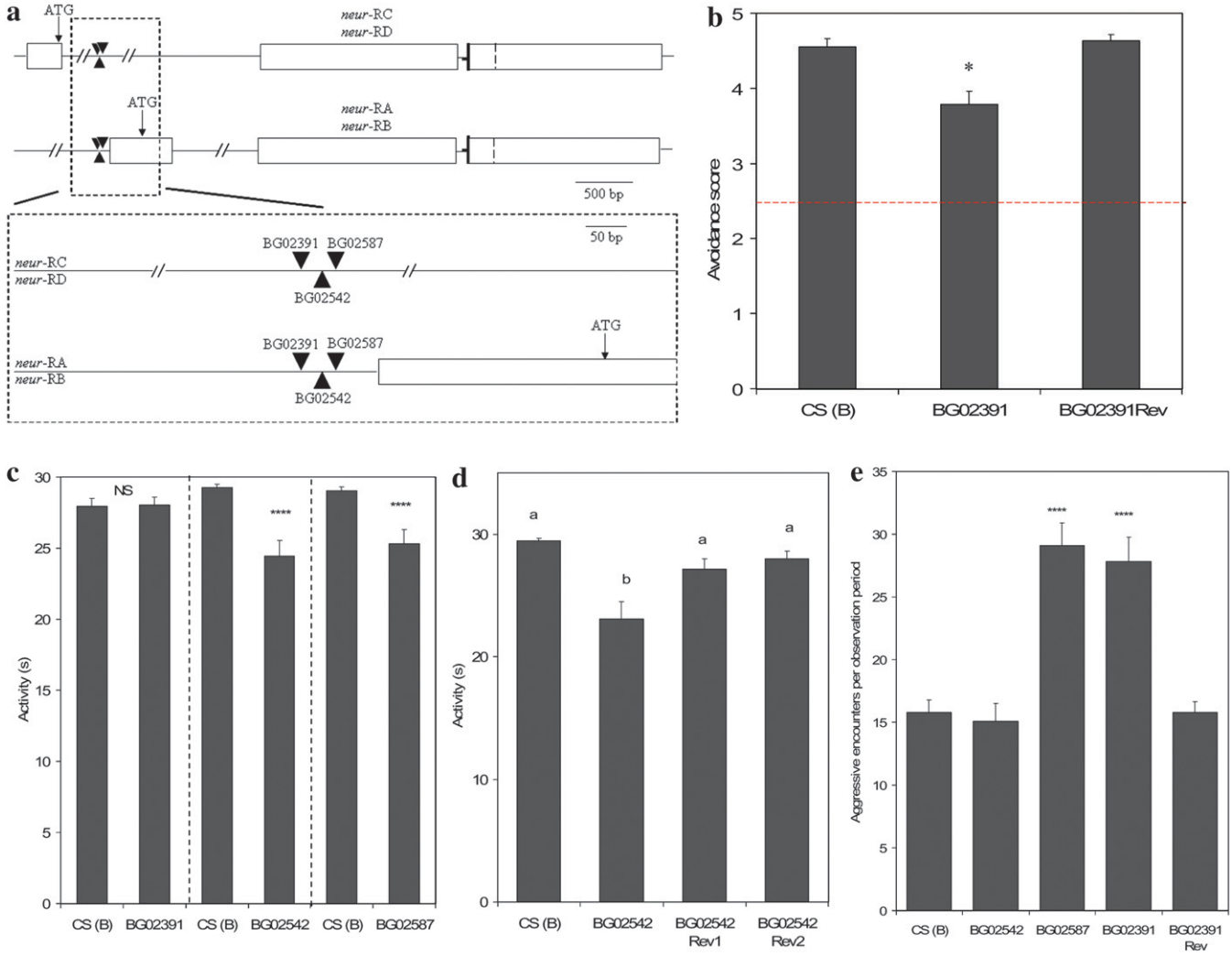

Figure 1.—Behavioral effects of transposon-mediated disruption of the *neur* gene. (a) *neur* gene structure and *P*-element insertion sites. The horizontal line represents genomic DNA with open boxes representing exons of *neur*. Alternative transcripts of *neur*-designated *neur*-RA, *neur*-RB, *neur*-RC, and *neur*-RD are shown with solid areas in intron 2 and exon 3 denoting small differences in the lengths of the transcripts. Three independent *p*[*GT1*] insertions in the first intron of *neur*-RC and *neur*-RD and upstream of the first exon of *neur*-RA and *neur*-RB were identified. *P*-element insertion sites are indicated by arrowheads. Translation initiation sites are denoted by ATG with an arrow. The end of the coding region is indicated by a vertical dashed line in exon 3. The inset shows a magnified view of the region containing the *P*-element insertion sites. Flanking sequences at the 3′-ends of the *P*-element insertions of BG02391 and BG02542 are CCAGTACTATCCGTTACTCTCCAGCTGAGCTGCGTCAGCGACGTCGCGC and CTCCAGCTGAGCTGCGTCAGCGACGTCGCGC, respectively. Flanking sequences at the 5′-ends of the *P*-element insertions of BG02542 and BG02587 are CAGTACTATCCGTTACT-CTCCAGCT and GCGCCAGTACTATCCGTTACTCTCCAGCTGAGCTG CGTCAGCGA, respectively. (b) Olfactory avoidance responses to benzaldehyde. The $neur^{BG02391}$ (BG02391) flies showed reduced behavioral avoidance responses to benzaldehyde. Excision of the *p*[*GT1*] construct (BG02391Rev) resulted in phenotypic reversion of olfactory avoidance behavior. The red dashed line denotes the expected avoidance score that corresponds to indifference to the presence of the odorant. Post-hoc Tukey's test was used to determine significant difference among line means; $*P < 0.05$. (c) Locomotor reactivity following mechanical stimulation. A significant reduction in locomotor reactivity was observed for $neur^{BG02542}$ (BG02542) and $neur^{BG02587}$ (BG02587). No significant difference was observed for $neur^{BG02391}$; $****P < 0.0001$. (d) Phenotypic reversion of locomotor reactivity after *P*-element excision. Locomotor reactivity was reduced in the *P*-element insertion line $neur^{BG02542}$ as compared to its Canton S (B) control. Precise excision of the *P* element in lines $neur^{BG02542Rev1}$ and $neur^{BG02542Rev2}$ restored locomotor reactivity to wild-type levels. Means designated by the same letter are not statistically significantly different from one another. (e) Aggressive behavior. A significant increase in aggressive encounters compared to the control was observed in $neur^{BG02391}$ and $neur^{BG02587}$. Excision of the *P* element (BG02391Rev) resulted in phenotypic reversion of aggressive encounters to wild-type Canton S (B) levels. $****P < 0.0001$ (post-hoc Tukey's test).

long-term memory formation, whereas short-term memory requires the gamma lobes (Zars *et al.* 2000; Pascual and Preat 2001; Yu *et al.* 2006). α- and β-lobe outputs serve in olfactory memory retrieval, but not in its formation or storage (Dubnau *et al.* 2001; McGuire *et al.* 2001; Schwaerzel *et al.* 2002). The ellipsoid body is also implicated in long-term memory consolidation (Wu *et al.* 2007). Here, we conducted morphological

TABLE 1

Effects of *P*-element insertions at the *neur* locus on average (± standard error) sternopleural and abdominal bristle numbers

Line	ST (♂ and ♀)	AB (♂)	AB (♀)
Canton S (B)	17.69 ± 0.22 (a, b)	17.8 ± 0.35 (a)	20.93 ± 0.32 (a)
$neur^{BG02391}$	15.85 ± 0.17 (c)	16.48 ± 0.31 (b)	20.13 ± 0.33 (a, b)
$neur^{BG02542}$	17.1 ± 0.18 (b)	17.38 ± 0.3 (a, b)	18.83 ± 0.37 (c)
$neur^{BG02587}$	18.3 ± 0.21 (a)	18.13 ± 0.31 (a)	19.43 ± 0.21 (b, c)
$neur^{BG02391Rev}$	17.33 ± 0.16 (b)	17.25 ± 0.23 (a, b)	19.93 ± 0.28 (a, b, c)

No difference between the sexes was observed for average sternopleural (ST) bristle number and therefore sternopleural bristle counts for the sexes were pooled. Significant differences were observed for the line-by-sex interaction for abdominal bristle (AB) number and therefore sexes were analyzed separately. Significant mean differences in bristle counts are designated by different lowercase letters (post-hoc Tukey's test).

and morphometric analyses of the ellipsoid body and the mushroom body α- and β-lobes of the adult brain following immunohistochemical labeling with the antifasciclin 2 antibody 1D4. This antibody strongly labels the α- and β-lobes of the mushroom bodies and, to a lesser extent, the gamma lobes (Figure 2a; Crittenden *et al.* 1998). We first determined whether any gross morphological alterations could be seen. Next we measured widths and lengths of the α- and β-lobes and diameters of the ellipsoid body. Mushroom bodies were scored individually (*i.e.*, per hemisphere) while ellipsoid body scores were scored per brain. A direct relationship between gross structural brain defects and behavior has been demonstrated previously (see, *e.g.*, Strauss 2002), but subtle alterations in brain neuroanatomy and behavioral changes have hardly been studied. The biological relevance of such subtle changes is illustrated by a recent study of the paper wasp, *Polistes instabilis*, where mushroom body volume was related to social aggression (Molina and O'Donnell 2007).

We observed gross morphological defects in some of the mushroom bodies of $neur^{BG02542}$ flies. These defects included shorter and thinner α-lobes (7/77; Figure 2b), missing α-lobes (2/77; Figure 2c), and aberrant projections of the α-lobe (1/77; Figure 2d). We did not observe such defects either in the co-isogenic controls (0/43) or in the $neur^{BG02391}$ (0/75) and $neur^{BG02587}$ (0/74) alleles. A *G*-test of independence (Sokal and Rohlf 1995) indicates that the frequency of aberrations is significantly different for the different genotypes ($G_3 = 26.04$, $P = 9.35 \times 10^{-6}$). In the central complex, the antifasciclin 2 antibody stains primarily the ellipsoid body, which is labeled in a characteristic pattern of two concentric rings (Figure 2e). We observed disorganized ellipsoid bodies (ranging from less distinct or poorly defined concentric rings to completely abnormal organization) or defects (ventral open) in 20 of 39 brains (Figure 2f) in the $neur^{BG02542}$ mutants. A comparable disorganization or poor structural definition but not the ventral open defect is occasionally observed in the wild-type control (4/22). We also did not see major disorganization in the $neur^{BG02391}$ (0/39) and $neur^{BG02587}$ (0/38) alleles. Again, a *G*-test reveals that the differences in frequency of ellipsoid body aberrations among these genotypes are significant ($G_3 = 56.60$, $P = 3.12 \times 10^{-12}$).

Whereas gross morphological defects were not always apparent, a detailed morphometric analysis revealed consistent subtle differences in neuroanatomical organization. We quantified widths and lengths of α- and β-lobes as well as surface areas of the ellipsoid bodies using the variables outlined in Figure 2g. To control for possible shrinkage effects due to fixation, all measurements were expressed as percentages relative to the distance between the two mushroom body heels (blue double arrow in Figure 2g). Behavioral alterations in the *neur* mutants reveal remarkable parallels with most neuroanatomical alterations. We found significant differences in α-lobe ($F_{6,327} = 2.991$; $P = 0.007$) and β-lobe widths ($F_{6,327} = 4.925$; $P < 0.001$). α- and β-lobe widths of $neur^{BG02391}$, which shows reduced olfactory responsiveness (Figure 1b) and hyperaggression (Figure 1e), were significantly different from the Canton-S (B) controls ($P < 0.05$; Figure 2i). Length measurements showed significant differences only for α-lobes ($F_{6,327} = 6.420$; $P < 0.001$). The α-lobe lengths of $neur^{BG02391}$ were significantly different from controls ($P < 0.05$) (Figure 2j). The analysis of ellipsoid body surfaces also revealed significant differences among *neur* alleles ($F_{6,165} = 2.153$; $P = 0.050$). The locomotor response-impaired $neur^{BG02542}$ mutant (Figure 1c) displayed a significantly reduced ellipsoid body surface relative to the Canton-S (B) control ($P < 0.05$). The other two *neur* alleles also showed a reduction in ellipsoid body surface, of which $neur^{BG02391}$ was also significantly different from Canton-S (B) (Figure 2k). We next asked whether the restoration of behavior to wild type seen for the $neur^{BG02391Rev}$, $neur^{BG02542Rev1}$, and $neur^{BG02542Rev2}$ alleles is accompanied by changes in morphology of mushroom bodies and ellipsoid bodies. None of the revertants displayed the gross morphological defects seen in the original alleles. Furthermore, we observed restoration of α- and β-lobe width as well as of ellipsoid body surface of $neur^{BG02391Rev}$

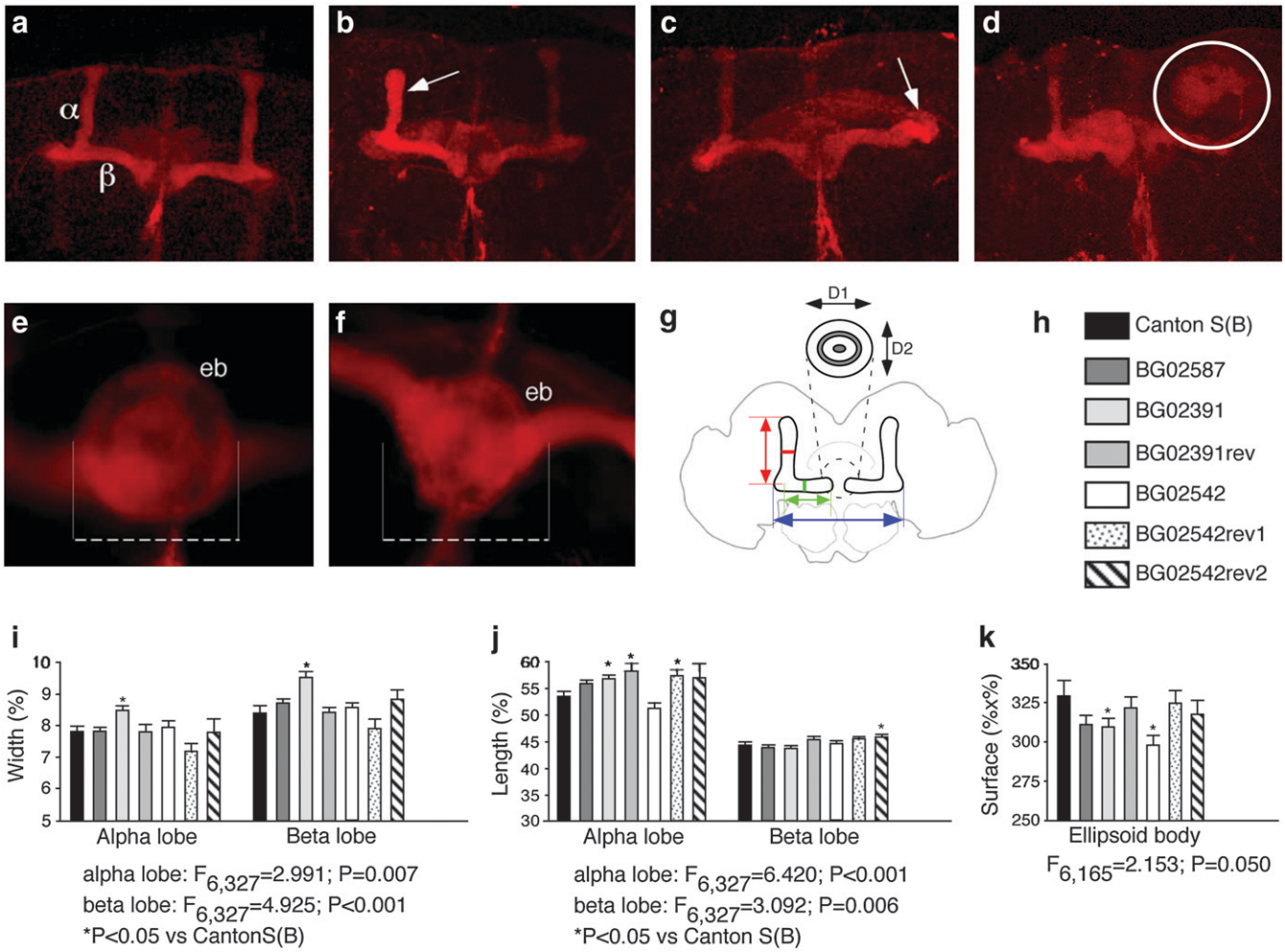

FIGURE 2.—Morphometric analysis of wild-type Canton S (B) controls and the *P*-element-tagged *neuralized* alleles BG02542, BG02391, and BG02587. (a–f) Antifasciclin 2 staining of adult brains using the 1D4 monoclonal antibody. (a) Canton S (B) control: α, α-lobes of mushroom bodies; β, β-lobes of mushroom bodies. (b–d) Mushroom body defects observed in $neur^{BG02542}$: short and thinner α-lobe (arrow in b); α-lobe missing (arrow in c); aberrant ball-shaped axonal projections instead of regular α-lobe (d). (e) Canton S (B) control: typical appearance of the ellipsoid body (eb) upon staining with antifasciclin 2 antibody reveals two concentric rings. (f) The ellipsoid body in $neur^{BG02542}$ often appears less organized and smaller. The dashed lines in e and f, which are at the same magnification, are of the same length, illustrating the fact that the ellipsoid body in $neur^{BG02542}$ is smaller. (g) Schematic of the measurements that were made for morphometry. α- and β-lobe diameters (red and green arrows, respectively) were measured and diameters D1 and D2 were determined for the ellipsoid body to calculate the ellipsoid body surface. The blue arrow indicates the distance between the α-lobe heels that was used to normalize the measurements for each brain. (h) Key for histograms in i–k. (i) Mushroom body α- and β-lobe widths in Canton S (B), $neur^{BG02542}$, $neur^{BG02391}$, $neur^{BG02587}$, $neur^{BG02542Rev1,2}$, and $neur^{BG02391Rev}$. (j) Mushroom body α- and β-lobe lengths in Canton S (B), $neur^{BG02542}$, $neur^{BG02391}$, $neur^{BG02587}$, $neur^{BG02542Rev1,2}$, and $neur^{BG02391Rev}$. (k) Ellipsoid body surfaces in Canton S (B), $neur^{BG02542}$, $neur^{BG02391}$, $neur^{BG02587}$, $neur^{BG02542Rev1,2}$, and $neur^{BG02391Rev}$. For the Canton S (B) controls, 43 hemispheres were scored for mushroom body defects and 22 brains for ellipsoid body defects. For the *neur* alleles, we examined 77 brain hemispheres for mushroom body defects and 39 brains for ellipsoid body defects for $neur^{BG02542}$, 75 brain hemispheres and 39 brains for $neur^{BG02391}$, and 74 brain hemispheres and 38 brains for $neur^{BG02587}$. For the $neur^{BG02542Rev1,2}$ and $neur^{BG02391Rev}$ revertant alleles, we analyzed 22, 23, and 21 brain hemispheres and 11, 12, and 11 brains, respectively. Lobe width and length were normalized to the distance between the α-lobe heels and are expressed as percentages. The ellipsoid body surface values shown in the *y*-axis in k were calculated by multiplying the radii (R1 = D1/2 and R2 = D2/2) expressed as percentages after normalization. The constant value Π of the formula surface = Π × R1 × R2 was omitted from the calculation.

to levels not different from Canton-S (B) controls (see Figure 2, i and k). Furthermore, we found that the ellipsoid body surface of both revertants for $neur^{BG02542}$ is restored to the size of the Canton-S (B) control (see Figure 2k). The one parameter that did not revert to wild-type values in the revertant lines was α-lobe length. We do not know the underlying reason for this observation, but our data indicate that the α-lobe phenotype seen in $neur^{BG02391}$ does not depend on the *P*-element insertion. It was previously shown that $neur^{BG02542}$ is associated with locomotor reactivity deficits and $neur^{BG02391}$ with aggressive behavior. The observation

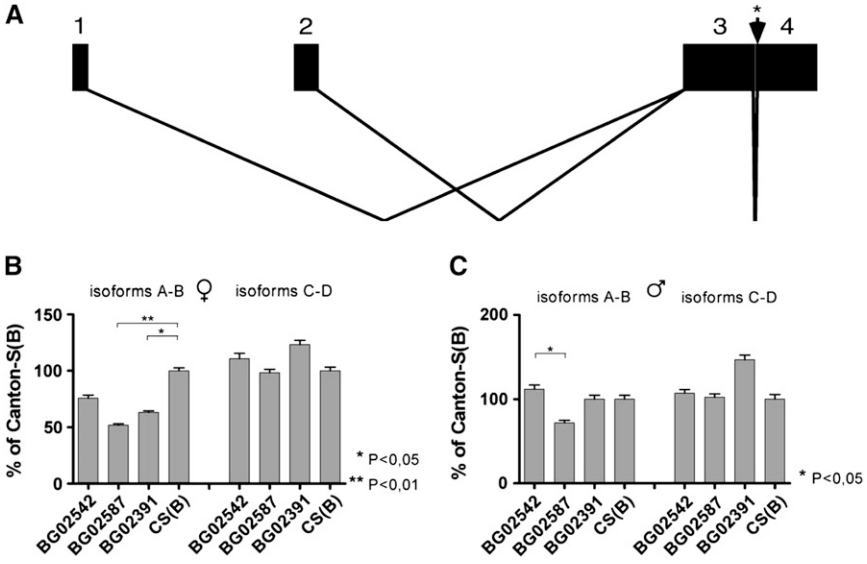

FIGURE 3.—qRT–PCR analysis of *neuralized* transcripts A-B and C-D in wild-type Canton S (B) controls and the *P*-element insertion alleles BG02542, BG02391 and BG02587. (A) Genomic structure of the *neuralized* gene. The *neuralized* gene consists of four exons (1–4). Alternative splice acceptor sites are located 3 bp apart at the 5′-end of exon 4 (arrow with asterisk; for the locations of the *P*-element insertion sites in the *neur* locus, see Figure 1a). (B) qRT–PCR analysis of A-B and C-D transcripts in RNA isolated from females of $neur^{BG02542}$, $neur^{BG02587}$, $neur^{BG02391}$, and Canton S (B). Transcript levels are expressed as percentages of the Canton S (B) control. The A-B transcript levels in $neur^{BG02587}$ and $neur^{BG02391}$ are significantly lower than in Canton S (B), whereas reduction in $neur^{BG02542}$ transcript levels does not reach statistical significance ($F_{3,8} = 11.399$; $P = 0.003$). The C-D transcripts do not differ. (C) qRT–PCR analysis of A-B and C-D transcripts in RNA isolated from males of $neur^{BG02542}$, $neur^{BG02587}$, $neur^{BG02391}$, and Canton S (B). Transcript levels are expressed as percentages of the Canton S (B) control. The A-B transcript levels in $neur^{BG02542}$ and $neur^{BG02587}$ differ significantly ($F_{3,8} = 4.570$; $P = 0.038$). The apparent reduction in the level of $neur^{BG02587}$ compared to $neur^{BG02391}$ and the Canton S (B) control is not statistically significant. For the C-D transcripts, no statistically significant differences were observed although the levels in $neur^{BG02391}$ appear higher. Statistical significance was determined with ANOVA and post-hoc analysis with Bonferroni correction.

that *P*-element excision results in reversion to wild-type levels of behavior and brain structure suggests that the alterations seen in the ellipsoid body and in ellipsoid body and mushroom body lobes, respectively, may be causally linked to the observed differences in behavior. This is consistent with the previously demonstrated roles of ellipsoid bodies and mushroom bodies in locomotor activity (MARTIN *et al.* 1998, 1999).

***P*-element insertions in *neuralized* affect ratios of alternative transcripts:** Small differences in the locations of the *P* elements might result in differences in expression levels or ratios of alternatively spliced transcripts which could impact different forms of adult behavior. To determine whether the different *P*-element insertions had differential effects on transcription, we performed qRT–PCR experiments, allowing us to discriminate transcripts A and B from transcripts C and D (Figure 3A). We found that there are indeed differential effects on these transcript pairs associated with the different *P*-element insertions (see Figure 3, B and C). This was most pronounced in females where transcripts A and B are significantly reduced in $neur^{BG02587}$ and $neur^{BG02391}$ when compared to the Canton-S (B) control. By contrast, no such differences were observed for the C and D transcripts in females. In males, a significant difference was seen between $neur^{BG02542}$ and $neur^{BG02587}$. The latter appears lower than $neur^{BG02391}$ and the Canton-S (B) control without, however, reaching statistical significance. The C and D transcripts again showed less variation although in $neur^{BG02391}$ an increase was seen that was, however, not statistically significant. These observations extend a previous study, in which we showed that *neur* transcript abundance is reduced in embryos and larvae of $neur^{BG02391}$ homozygotes and that this reduction resulted in decreased olfactory avoidance behavior in adult flies (SAMBANDAN *et al.* 2006).

Genes with altered transcriptional regulation in adult *neur* mutants: Previously, we showed that single *P*-element insertions cause genomewide alterations in expression of coregulated genes (ANHOLT *et al.* 2003). To determine to what extent the *p[GT1]*-element insertion alleles of *neur* alter the transcriptional context of *neur* expression, we examined genomewide transcriptional profiles in the Canton-S (B) control and $neur^{BG02391}$, $neur^{BG02542}$, and $neur^{BG02587}$ mutants using Affymetrix high-density oligonucleotide Drosophila GeneChips. Analysis of whole-genome transcriptional profiles resulted in 135 probe sets with altered expression levels at a false discovery rate of $q < 0.05$ (STOREY and TIBSHIRANI 2003; supplemental Table S1). We observed considerable overlap among the ensembles of genes with altered expression in the different mutants. Of the 135 probe sets, 85 (63%) were altered in two or more mutant lines compared to the co-isogenic Canton-S (B) control. However, 22 were altered only in $neur^{BG02391}$, 11 only in $neur^{BG02542}$, and 8 only in $neur^{BG02587}$, consistent with different behavioral, morphological, and neuroanatomical phenotypes observed for each mutant allele (supplemental Table S1). In addition, 9 lines showed a significant line-by-sex interaction (supplemental Tables S1 and S2). Precedence for such different phenotypic effects arising from nearby *P* elements, or even from *P* elements at the same insertion site but in different orientations, has been documented previously for *P*-element insertions in the

TABLE 2

Overrepresented gene ontology categories of coregulated transcripts in *neur* mutants

Biological process[a]	*P*	Genes
Carbohydrate metabolism (23)	2.80E−09	*Peptidoglycan-recognition protein-SC1a/b precursor, Amylase distal, Amylase proximal, Peptidoglycan-recognition protein-SD precursor, Lysozyme P, Lysozyme X, Lysozyme C, GIP-like, Lysozyme E, Peptidoglycan-recognition protein-S2 precursor, Isocitrate dehydrogenase, Serine pyruvate aminotransferase, Lyzozyme B,* 10 predicted transcripts
Hydrolase activity (43)[b]	1.40E−08	*Peptidoglycan-recognition protein-SC1a/b precursor, Amylase distal, Serine protease 6, Minichromosome maintenance 6, Serine protease 12, Amylase proximal, Lysozyme P, Peptidoglycan-recognition protein-SD precursor, GIP-like, Jonah 6Ci, Jonah 44E, Astray, Lysozyme C, Lysozyme X, Puromycin sensitive aminopeptidase, Jonah 74E, Lysozyme E, Tubulin at 67C, Jonah 65Ai, Peptidoglycan-recognition protein-SC2 precursor, Alkaline phosphatase 4, Lysozyme B,* 20 predicted transcripts
Antibacterial humoral response (8)	1.70E−07	*Cecropin A1, Attacin-D, Lysozyme P, Lysozyme B, Lysozyme C, Lysozyme X, Lysozyme E, Peptidoglycan-recognition protein-SD precursor*
Chymotrypsin activity (12)[b]	6.20E−07	*Serine protease 6, Jonah 66Ci, Jonah 65Ai, Jonah 44E, Serine protease 12, Jonah 74E,* 6 predicted transcripts
Immune response (10)	1.90E−06	*Peptidoglycan-recognition protein-SC1a/b precursor, Cecropin A1, Attacin-D Peptidoglycan-recognition protein-SC2 precursor, Lysozyme P, Lysozyme B, Peptidoglycan-recognition protein-SD precursor, Lysozyme C, Lysozyme X, Lysozyme E*

Analyses were performed with the DAVID program (Dennis *et al.* 2003) and the complete data output is presented in supplemental Table 3.

[a] The number of coregulated transcripts in each category is indicated in parentheses.

[b] The *jonah* genes indicated in this category are annotated as serine-type peptidases.

Tre1-Gr5a region that differentially affect starvation and heat stress resistance, gustatory behavior, and life span (Rollmann *et al.* 2006). In addition, 9 probe sets showed sex-specific differences in expression (supplemental Table S2). It is of interest that, among the genes with altered transcriptional regulation in one or both of our hyperaggressive *neur* mutants, 34 exhibited differential regulation in lines selected for increased or decreased aggression (Edwards *et al.* 2006; <15 genes would be expected by chance).

We assigned coregulated genes to the gene ontology categories of molecular function and biological process (Dennis *et al.* 2003). The five most significant biological process categories are highlighted in Table 2 and the complete data set is presented in supplemental Table S3. In contrast to transcripts expected to be associated with the function of *neur* in early development of the nervous system, such as *Notch* and *Delta*, transcripts with altered regulation in the *neur* mutant background in adult flies are predominantly associated with proteolysis. This is in line with the ubiquitin ligase function of the *neur* gene product and could reflect a role in the dynamics of synaptic organization, as implied previously for *Tequila*, which is transiently upregulated in the mushroom bodies during memory formation (Didelot *et al.* 2006) and shows altered regulation in the *neur* mutants.

DISCUSSION

We have shown that distinct *P*-element insertions at nearby locations in the *neur* gene give rise to profoundly different effects on adult behaviors and that aberrant startle-induced locomotor responses, olfactory responses, and aggression correlate with different structural alterations in integrative brain centers, the mushroom bodies, and the ellipsoid body of the central complex. Similar pleiotropic allelic effects with differential effects on life span, resistance to heat stress and starvation, and preference for trehalose intake were observed previously for *P*-element insertions in the *Tre1-Gr5a* region (Rollmann *et al.* 2006). In addition, different naturally occurring polymorphisms in *Catsup*, which encodes a negative regulator of tyrosine hydroxylase, are associated with phenotypic variation in sternopleural bristle number, environmental plasticity of abdominal bristle number, and starvation resistance (Carbone *et al.* 2006). The diverse phenotypic effects arising from nearby *P*-element insertions in *neur* contribute to an emerging new appreciation of the concept of allelic effects on phenotype, in which the wild type and null mutant are at the extreme ends of a continuum of pleiotropic allelic effects. Subtle alterations in transcript abundance for splice variants may contribute to these pleiotropic effects, which would be in line with the subtle regulatory variations that have been associated with phenotypic effects on human and rodent behaviors (*e.g.*, Krishnan *et al.* 2007; Jensen *et al.* 2008).

Previous studies have shown that the introduction of a single *P*-element in the genome gives rise to widespread altered transcriptional regulation and that about two-thirds of genes with altered transcriptional regulation in a *P*-element-disrupted background are candidate genes

affecting the trait (Anholt *et al.* 2003). Moreover, such altered transcriptional profiles can define a functional context for the disrupted gene (Rollmann *et al.* 2005). The results from our expression microarray analysis show that insertions of *P* elements in *neur* result in a genomewide cascade of transcripts with altered expression. Proteolytic and degradative enzymes feature prominently among coregulated genes. One protease-encoding transcript that features notably in these transcriptional profiles is *Tequila*, which has previously been implicated in synaptic plasticity in the mushroom bodies during memory formation (Didelot *et al.* 2006; supplemental Table S3). One could speculate that the different, yet overlapping patterns of transcriptional profiles with altered expression of proteolytic enzymes and peptidoglycan recognition precursor proteins (Table 2) may reflect alterations in neural connectivity, which could contribute to the different behavioral effects. In addition, changes in structure of the mushroom bodies and ellipsoid body could also arise from developmental effects of *neuralized* (Sambandan *et al.* 2006).

The behavioral phenotypes of *neur* mutant flies are reminiscent of those encountered in patients suffering from neuropsychiatric and neurodegenerative disorders, including reduced responsiveness to environmental stimuli and increased aggressive behavior. Neurodegenerative and neuropsychiatric disorders ranging from bipolar disorder, schizophrenia, and antisocial personality disorder to Alzheimer's and Parkinson's disease are often accompanied by behavioral alterations, such as indifference to stimuli, hypokinesia, hyperactivity, and aggression (Paveza *et al.* 1992; Aarsland *et al.* 1999; Moran 1999; Oquendo *et al.* 2000; Brieden *et al.* 2002; Haller and Kruk 2006). Apathy and aggressive behavior have a catastrophic impact on the social functioning of neuropsychiatric patients. In addition, these behaviors represent some of the most difficult to treat symptoms. Whereas it is likely that underlying genetic architectures that may predispose to such behavioral syndromes are heterogeneous and complex, we have demonstrated that reduced responsiveness to environmental stimuli together with increased aggressive behavior can arise from a single hypomorphic mutation at the *neur* locus in Drosophila and that these behavioral defects are associated with distinct subtle alterations in neuroanatomy.

We thank Richard Lyman for assistance in the analysis of bristle phenotypes, Stefanie Heinsohn and Stacy Williams for technical assistance, Ann Schellens for help with the qRT–PCR analyses, Mimi Deprez for help with preparing the figures and Zsuzsanna Callaerts-Vegh for help with the statistical analysis of the morphometric and qRT–PCR data. K.N. is a Senior Clinical Investigator of the Fonds voor Wetenschappelÿk Onderzoek-Flanders. L.Z. is supported by the Institute for the Promotion of Innovation through Science and Technology in Flanders (Instituut voor de Aanmoediging van Innovatie door Wetenschap en Technologie in Vlaandeven). This work was supported by grants from the National Institutes of Health (to R.R.H.A. and T.F.C.M.) and in part by a Belgian Federal Science Policy Return Grant (to K.N.), a Marie-Curie International Reintegration Grant (to K.N.), and Vlaams Instituut voor Biotechnologie. This is a publication of the W. M. Keck Center for Behavioral Biology at North Carolina State University.

LITERATURE CITED

Aarsland, D., J. P. Larsen, N. G. Lim, C. Janvin, K. Karlsen *et al.*, 1999 Range of neuropsychiatric disturbances in patients with Parkinson's disease. J. Neurol. Neurosurg. Psychiatry **67:** 492–496.

Anholt, R. R. H., 2004 Genetic modules and networks for behavior: lessons from *Drosophila*. BioEssays **26:** 1299–1306.

Anholt, R. R. H., R. F. Lyman and T. F. C. Mackay, 1996 Effects of single *P*-element insertions on olfactory behavior in *Drosophila melanogaster*. Genetics **143:** 293–301.

Anholt, R. R. H., C. L. Dilda, S. Chang, J. J. Fanara, N. H. Kulkarni *et al.*, 2003 The genetic architecture of odor-guided behaviour in *Drosophila*: epistasis and the transcriptome. Nat. Genet. **35:** 180–184.

Bellen, H. J., R. W. Levis, G. Liao, Y. He, J. W. Carlson *et al.*, 2004 The BDGP gene disruption project: single transposon insertions associated with 40% of Drosophila genes. Genetics **167:** 761–781.

Brieden, T., M. Ujeyl and D. Naber, 2002 Psychopharmacological treatment of aggression in schizophrenic patients. Pharmacopsychiatry **35:** 83–89.

Carbone, M. A., K. W. Jordan, R. F. Lyman, S. T. Harbison, J. Leips *et al.*, 2006 Phenotypic variation and natural selection at *Catsup*, a pleiotropic quantitative trait gene in *Drosophila*. Curr. Biol. **16:** 912–919.

Crittenden, J. R., E. M. Skoulakis, K. A. Han, D. Kalderon and R. L. Davis, 1998 Tripartite mushroom body architecture revealed by antigenic markers. Learn. Mem. **5:** 38–51.

Dennis, G., Jr., B. T. Sherman, D. A. Hosack, J. Yang, W. Gao *et al.*, 2003 DAVID: database for annotation, visualization and integrated Discovery. Genome Biol. **4:** 3.

Didelot, G., F. Molinari, P. Tchenio, D. Comas, E. Milhiet *et al.*, 2006 Tequila, a neurotrypsin ortholog, regulates long-term memory formation in Drosophila. Science **313:** 851–853.

Dietrich, U., and J. A. Campos-Ortega, 1984 The expression of neurogenic loci in imaginal epidermal cells of *Drosophila melanogaster*. J. Neurogenet. **1:** 315–332.

Dubnau, J., L. Grady, T. Kitamoto and T. Tully, 2001 Disruption of neurotransmission in *Drosophila* mushroom body blocks retrieval but not acquisition of memory. Nature **411:** 476–480.

Edwards, A. C., S. M. Rollmann, T. J. Morgan and T. F. C. Mackay, 2006 Quantitative genomics of aggressive behavior in *Drosophila melanogaster*. PLoS Genet. **2:** 1386–1395.

Haller, J., and M. Kruk, 2006 Normal and abnormal aggression: human disorders and novel laboratory models. Neurosci. Biobehav. Rev. **30:** 292–303.

Jensen, K. P., J. Covault, T. S. Conner, H. Tennen, H. R. Kranzler *et al.*, 2008 A common polymorphism in serotonin receptor 1B mRNA moderates regulation by miR-96 and associates with aggressive human behaviors. Mol. Psychiatry (in press).

Jordan, K. W., T. J. Morgan and T. F. C. Mackay, 2006 Quantitative trait loci for locomotor behavior in *Drosophila melanogaster*. Genetics **174:** 271–284.

Krishnan, V., M. H. Han, D. L. Graham, O. Berton, W. Renthal *et al.*, 2007 Molecular adaptations underlying susceptibility and resistance to social defeat in brain reward regions. Cell **131:** 391–404.

Lai, E. C., and G. M. Rubin, 2001 *neuralized* is essential for a subset of Notch pathway-dependent cell fate decisions during *Drosophila* eye development. Proc. Natl. Acad. Sci. USA **98:** 5637–5642.

Lai, E. C., G. A. Deblandre, C. Kintner and G. M. Rubin, 2001 *Drosophila neuralized* is a ubiquitin ligase that promotes the internalization and degradation of delta. Dev. Cell **1:** 783–794.

Lukacsovich, T., Z. Asztalos, W. Awano, K. Baba, S. Kondo *et al.*, 2001 Dual-tagging gene trap of novel genes in *Drosophila melanogaster*. Genetics **157:** 727–742.

Martin, J. R., R. Ernst and M. Heisenberg, 1998 Mushroom bodies suppress locomotor activity in *Drosophila melanogaster*. Learn. Mem. **5:** 179–191.

Martin, J. R., T. Raabe and M. Heisenberg, 1999 Central complex substructures are required for the maintenance of locomotor activity in *Drosophila melanogaster*. J. Comp. Physiol. A **185:** 277–288.

McGuire, S. E., P. T. Le and R. L. Davis, 2001 The role of *Drosophila* mushroom body signaling in olfactory memory. Science **293:** 1330–1333.

Molina, Y., and S. O'Donnell, 2007 Mushroom body volume is related to social aggression and ovary development in the paperwasp *Polistes instabilis*. Brain Behav. Evol. **70:** 137–144.

Moran, P., 1999 Epidemiology of antisocial personality disorder. Soc. Psychiatry Psychiatr. Epidemiol. **34:** 231–242.

Norga, K. K., M. C. Gurganus, C. L. Dilda, A. Yamamoto, R. F. Lyman *et al.*, 2003 Quantitative analysis of bristle number in *Drosophila* mutants identifies genes involved in neural development. Curr. Biol. **13:** 1388–1396.

Oquendo, M. A., C. Waternaux, B. Brodsky, B. Parsons, G. L. Haas *et al.*, 2000 Suicidal behavior in bipolar mood disorder: clinical characteristics of attempters and nonattempters. J. Affect. Disord. **59:** 107–117.

Pascual, A., and T. Preat, 2001 Localization of long-term memory within the *Drosophila* mushroom body. Science **294:** 1115–1117.

Paveza, G. J., D. Cohen, C. Eisdorfer, S. Freels, T. Semla *et al.*, 1992 Severe family violence and Alzheimer's disease: prevalence and risk factors. Gerontologist **32:** 493–497.

Pavlopoulos, E., C. Pitsouli, K. M. Klueg, M. A. Muskavitch, N. K. Moschonas *et al.*, 2001 *neuralized* encodes a peripheral membrane protein involved in delta signaling and endocytosis. Dev. Cell **1:** 807–816.

Rollmann, S. M., T. F. C. Mackay and R. R. H. Anholt, 2005 Pinocchio, a novel protein expressed in the antenna, contributes to olfactory behavior in *Drosophila melanogaster*. J. Neurobiol. **63:** 146–158.

Rollmann, S. M., M. M. Magwire, T. J. Morgan, E. D. Ozsoy, A. Yamamoto *et al.*, 2006 Pleiotropic fitness effects of the *Tre1-Gr5a* region in *Drosophila melanogaster*. Nat. Genet. **38:** 824–829.

Sambandan, D., A. Yamamoto, J. J. Fanara, T. F. C. Mackay and R. R. H. Anholt, 2006 Dynamic genetic interactions determine odor-guided behavior in *Drosophila melanogaster*. Genetics **174:** 1349–1363.

Schwaerzel, M., M. Heisenberg and T. Zars, 2002 Extinction antagonizes olfactory memory at the subcellular level. Neuron **35:** 951–960.

Sokal, R. R., and F. J. Rohlf, 1995 *Biometry*, Ed. 3. W. H. Freeman, New York.

Storey, J. D., and R. Tibshirani, 2003 Statistical significance for genome-wide studies. Proc. Natl. Acad. Sci. USA **100:** 9440–9445.

Strauss, R, 2002 The central complex and the genetic dissection of locomotor behaviour. Curr. Opin. Neurobiol. **12:** 633–638.

Timmusk, T., K. Palm, N. Belluardo, G. Mudo and T. Neuman, 2002 Dendritic localization of mammalian *neuralized* mRNA encoding a protein with transcription repression activities. Mol. Cell. Neurosci. **20:** 649–668.

van Swinderen, B., and R. J. Greenspan, 2005 Flexibility in a gene network affecting a simple behavior in *Drosophila melanogaster*. Genetics **169:** 2151–2163.

Wu, C.-L., S. Xia, T.-F. Fu, H. Wang, Y.-H. Chen *et al.*, 2007 Specific requirement of NMDA receptors for long-term memory consolidation in *Drosophila* ellipsoid body. Nat. Neurosci. **10:** 1578–1586.

Yeh, E., L. Zhou, N. Rudzik and G. L. Boulianne, 2000 Neuralized functions cell autonomously to regulate *Drosophila* sense organ development. EMBO J. **19:** 4827–4837.

Yu, D., D.-B.G. Akalal and R.L. Davis, 2006 *Drosophila* α/β mushroom body neurons form a branch-specific, long-term cellular memory trace after spaced olfactory conditioning. Neuron **52:** 845–855.

Zars, T., M. Fischer, R. Schulz and M. Heisenberg, 2000 Localization of a short-term memory in *Drosophila*. Science **288:** 672–675.

Communicating editor: L. Harshman